ON THE NATURE OF CARBON STARS WITH THE PROMISE OF FIRST

S.J. Chan

Space Science Department, Rutherford Appleton Laboratory, Chilton, Didcot, Oxon, OX11 0QX, UK

Abstract

A set of self-consistent model calculations of the evolution from visual carbon stars to infrared carbon stars is presented and reviewed. A two-shell system model, the *interrupted mass–loss model*, has been developed. A revised mass-loss formula, which describes the gradually increasing mass-loss rate at the early stage of the infrared carbon stars, is introduced to simulate the effect of the newly-forming SiC shell. The model tracks successfully explain a 'C'-shaped distribution of carbon stars in the colour-colour diagram. The existence of these transition objects with infrared properties intermediate between visual and infrared carbon stars, lends further support to the idea of an evolutionary link between visual and infrared carbon stars. FIRST mission will be played an important role for the detailed study of the nature of carbon stars.

Key words: Stars: evolution of – Stars: carbon – Stars: circumstellar matter – Stars: mass loss – infrared radiation

1. Introduction

The discovery of far infrared excesses in visual carbon stars (Thronson et al. 1987) has led to the 'theory' that visual carbon stars (stars were identified from optical surveys) descend from mass-losing oxygen-rich stars and the excess is due to the remnant of the oxygen-rich silicate dust shell (Chan & Kwok 1988, hereafter referred CK1). The distribution of visual carbon stars in the IRAS colour-colour diagram can be successfully explained by this 'detached-shell' model. On the other hand, infrared carbon stars (stars with circumstellar SiC features) have a distribution in the colour-colour diagram along the blackbody line, and they are currently undergoing large-scale mass loss (Chan & Kwok 1990, hereafter referred CK2).

Assuming that visual carbon stars evolve into infrared carbon stars, there remains a group of transition objects distributed in the shape of a 'C' between the visual and infrared carbon stars in the IRAS colour-colour diagram. In order to model these transition objects, we need to take into account both the remnant silicate dust shell, and the newly-forming SiC dust shell.

In this paper, a two-shell system model (the interrupted mass-loss model) with an oxygen-rich detached shell and a newly-forming SiC dust shell is presented and reviewed. The energy distributions generated by the model are compared with available data of these transition objects (such as ISO–LWS, IRAS–LRS, IRAS–PSC, near-infrared and optical photometry).

2. Selecting the working sample

The stars selected as the working sample should be the main members forming the shape of a 'C' in the colour-colour diagram. Their IRAS-LRS spectra should be available and also should show a weak SiC feature or be featureless. The featureless objects can be interpreted as being in the stage before the new shell starts to form or in the new shell phase at a very early formation stage. 372 visual carbon stars were selected as the working sample.

3. Interrupted mass loss model

3.1. Mass loss formula for a forming shell

In order to simulate the effect of the newly-forming SiC shell, the mass-loss rate at the early stage of infrared carbon star has to increase gradually, is assumed. The basic assumption is the following: the new mass-loss rate $\dot{\mathrm{M}}_{\mathrm{new}}(\mathrm{t})$ gradually increases until its value approaches a steady-state value $\dot{\mathrm{M}}_{\mathrm{o}}(\mathrm{new})$. Since the relationship between $\dot{\mathrm{M}}_{\mathrm{o}}(\mathrm{new})$ and the optical depth $\tau_{\lambda_{\mathrm{s}}}$($\lambda_s$ is the reference wavelength of SiC opacity function, i.e. 11.3 μm) is linear, from Eqn. 2 in CK2, the optical depth of the new shell $\tau_{\lambda_s}(\mathrm{new})(\mathrm{r,t})$ also approaches a steady-state value $\tau_{\lambda_{\mathrm{s}}}$, which corresponds to $\dot{\mathrm{M}}_{\mathrm{o}}(\mathrm{new})$. At some time when $\tau_{\lambda_{\mathrm{s}}}(\mathrm{new})(\mathrm{r,t})$ is nearly equal $\tau_{\lambda_{\mathrm{s}}}$, the dust shell is taken to be completed formed. The mass loss $\dot{\mathrm{M}}_{\mathrm{new}}(\mathrm{t})$ at time t is assumed to be

$$\dot{\mathrm{M}}_{\mathrm{new}}(\mathrm{t}) = \begin{cases} \dot{\mathrm{M}}_{\mathrm{o}}(\mathrm{new})(1-\mathrm{e}^{-\alpha(\mathrm{t}-\Delta\mathrm{t})}), & \mathrm{t} \geq \Delta\mathrm{t} + \frac{\mathrm{r_o(new)}}{\mathrm{v}} \\ \dot{\mathrm{M}}_{\mathrm{o}}(\mathrm{new}), & \mathrm{t} > 6\alpha^{-1} + \Delta\mathrm{t} \end{cases}$$

where α is a growth factor which controls the rate of the formation of the SiC shell. Δt is an interruption time interval which is defined as the time interval between when the old shell starts to detach and the new shell starts to form. r_o(new) is the condensation radius of the new SiC shell. 'v' is the expansion speed of the new shell. The density profile of the new dust shell is of the form

$$\rho(\mathrm{r,t}) \propto \frac{1-\mathrm{e}^{-\alpha(\mathrm{t}-\mathrm{r}/\mathrm{v}-\Delta\mathrm{t})}}{\mathrm{r}^2} \qquad \mathrm{t} - \tfrac{\mathrm{r}}{\mathrm{v}} - \Delta\mathrm{t} \geq 0$$

Proc. Symposium *'The Promise of the Herschel Space Observatory'* 12–15 December 2000, Toledo, Spain
ESA SP-460, July 2001, eds. G.L. Pilbratt, J. Cernicharo, A.M. Heras, T. Prusti, & R. Harris

The r/v factor is for the effect of the propagation time in the shell.

3.2. Two-shell system

To construct a model for a two-shell system, the values of emergent intensities and flux produced by the single new shell models were used as boundary conditions for the inner edge of the second dust shell. The growth factor, $\alpha \sim 5$ x 10^{-4} yr^{-1} and the interuption time interval, $\Delta t \sim$ 3000 yr or 5000 yr were chosen respectively. The expansion velocity of both the new shell and the old shell is assumed to be 10 km/s. Further, the stellar temperature is assumed to be $T_* = 2500$ K or $T_* = 2250$ K. The time steps (t - Δt, the age of the new shell) of each run range from 10 yr to 3x10^4 yr in most cases. The input dust parameters of the two-shell system are the same as those in CK1 and CK2.

The radiative transfer program was adapted from DUSTCD3 code (Egan et al 1988). Given the stellar wind properties, the density profile of the dust can be produced. the equation of radiative transfer is solved by an iterative method to obtain the source function at each part of the shell. The steady-state temperature profile and total emergent flux for the dust cloud are then calculated from the source function.

4. Results

4.1. The evolution of model spectra

The evolutionary tracks start in the area of the colour-colour diagram populated by the visual carbon stars (see Figure 2 in Chan 1993). The tracks have shapes like a 'C' of various sizes, which pass through the colour-points of most of the visual carbon stars. This is particularly successful in explaining many of the carbon stars which have very large 60 μm excesses and also have a weak SiC feature. Eventually, after the order of 3 x 10^4 yr, the tracks end on the assumed colour point corresponding to $\tau_{11.3\mu m}$(new) ~ 0.75 at which the 11.3 μm emission feature is a maximum.

At this point, the new SiC dust shell is considered to be completely formed, and the old shell is considered to be completely detached. The evolution of the model spectra from $\sim$ 3010 yr to 3x10^4 yr (with Δt = 3000 yr) are shown in Figure 1 and Figure 2 at different $\tau_{11.3\mu m}$(total). We note that the contribution of the expanding shell to the total energy distribution shifts to longer wavelengths as time goes on. Therefore, the old expanding shell gives rise to a 60 μm excess. At the same time, the 11.3 μm feature becomes stronger and stronger as the new shell grows. After less than age 10^3 yr, the effect of the 60 μm excess from the old shell is overcome by the effect of the increasing circumstellar emission at 60 μm of the new shell. Eventually, there is little difference between the model spectra of a two-shell system and of a single SiC shell system.

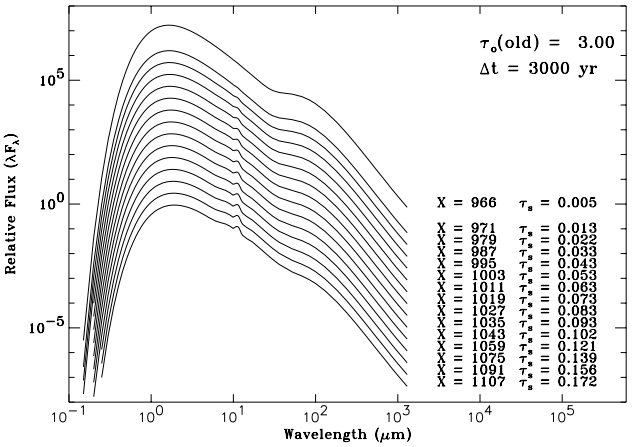

Figure 1. The evolution of the model spectra of the interrupted mass-loss model with Δt=3000 yr and $\tau_{10\mu u}$(old) = 3.0 from X=966 (where x=r/r_o) to 1107.

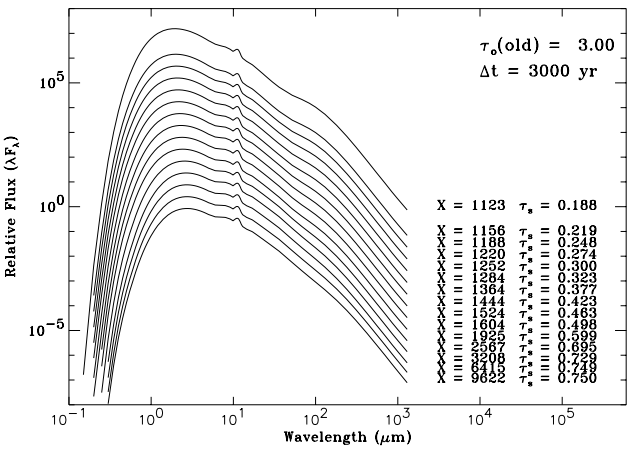

Figure 2. The evolution of the model spectra of the interrupted mass-loss model with Δt=3000 yr and $\tau_{10\mu u}$(old) = 3.0 from X=1123 to 9622.

4.2. The model spectra via the observed data

The energy distributions are then compared with the overall energy distributions of specific objects. For some objects in the working sample, further observational data in the ISO-LWS, IRAS-LRS plus optical, near-infrared, and IRAS photometry are available. Figures (see Figure 3, 4 and 5) show three examples of the model fits to the observed data. Optical photometry (U, B, V) is taken from the *General Catalog of Cool Galactic Carbon Stars*, 2nd ed. (Stephenson 1989) and the *Bright Star Catalog* (Hoffleit and Jascheck 1982), and the near-infrared photometry from Noguchi et al. (1981, 1990), Epchtein et al. (1987, 1990), Fouqué et al. (1992), *NASA Catalog of Infrared Observations* (Gezari et al. 1994), and *AFGL Catalog* (Price et al. 1976). About 66% of the objects are matched by the

model spectral with Δt=3000 yr. The remaining objects are fitted well by the model spectra with Δt=5000 yr. The energy distributions of ∼110 transition objects, which are in the late visual carbon star stage or in the early infrared carbon stars stage, are fitted well using the *interrupted mass-loss model*

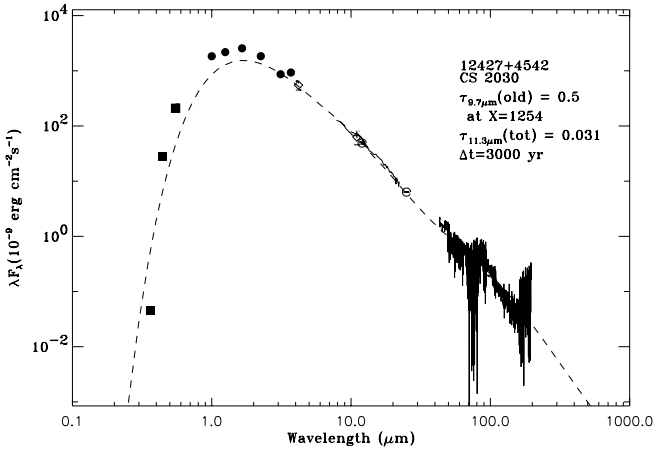

Figure 3. The energy distribution of Y CVn (IRAS 12427+4542).

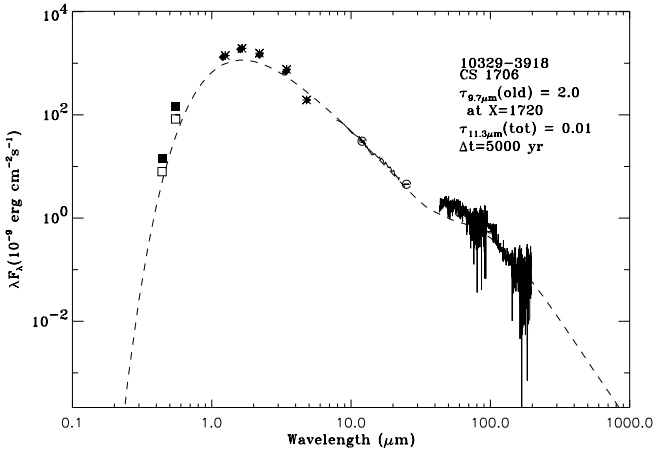

Figure 4. The energy distribution of U Ant (IRAS 10329-3918).

4.3. From visual to infrared carbon stars

The evolutionary tracks of the transition objects form the shape of a 'C' in the colour-colour diagram during the last stages of visual carbon star evolution, as the oxygen-rich shell disperses into the interstellar medium and the new SiC shell forms. Representative objects can be found to illustrate the above evolutionary scenario. These objects,

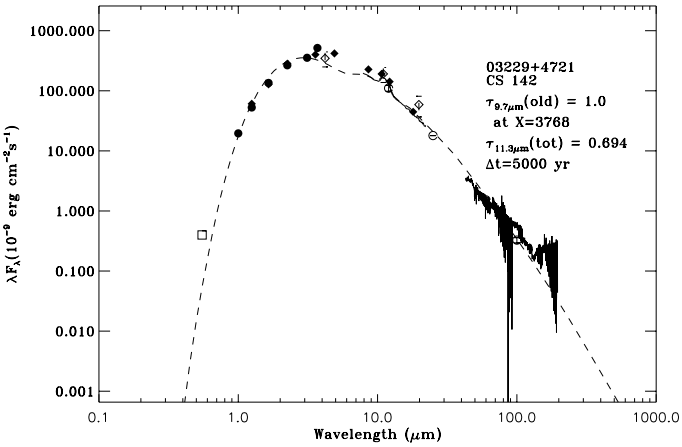

Figure 5. The energy distribution of IRC 50096 (IRAS 03229+4721).

which are fitted by the *interrupted mass-loss model* with the age of the new SiC shell less than 10^3yr, show the 11.3 μm SiC feature and at the same time display an excess at 60 μm. Therefore, they are candidates for objects in the process of evolving from visual carbon stars to infrared carbons.

As the mass-loss rate increases, the optical depth of the circumstallar envelope increase. IRC 50096 (IRAS 03229+4721, see figure 5) is a typical infrared carbon star. The photosphere is highly reddened, and the circumstellar dust continuum is dominant at $\lambda > 5\mu$m. There is also very little evidence of the remnant of the oxygen-rich shell in the form of a 60 μm excess. The SiC feature is prominent and easily identified. Furthermore, the *interrupted mass-loss model* spectrum fit to the observed energy distribution of IRC 50096, gives an age of new SiC shell of $\sim 10^4$yr.

5. Discussion

5.1. CO observations and ISO observations

Recent CO observations have led to the detection of many visual carbon stars (Olofsson et al. 1990, 1992, 1996). These detections confirm that visual carbon stars possess expanding circumstellar shells as suggested by their 60 μm excess. Moreover, the visual carbon stars S Scuti, U Antliae (IRAS 19390+3229; see figure 4) and TT Cygni were found to have double-peaked CO profiles which are interpreted by Olofsson et al. (1990, 1992, 1996) as being due to detached shells. These three objects are the candidates of the transition objects fitted well by the *interrupted mass-loss model*. The current mass-loss rates of S Sct given by Olofsson et al. (1992) and Yamamura et al. (1993) are 3.0×10^{-8}M$_\odot$yr^{-1} and 1.2×10^{-8}M$_\odot$yr^{-1}, respectively. The value determined from the present model is $\sim 1.5 \times 10^{-8}$M$_\odot$yr^{-1}, whereas the mass-loss rate for

the old shell is $\sim 3.9 \times 10^{-6} M_{\odot} yr^{-1}$. The value determined by Olofsson et al (1996) is $\sim 3.0 \times 10^{-5} M_{\odot} yr^{-1}$. The present mass-loss rate of U Ant estimated by Olofsson et al.(1996) is $\leq 10^{-7} M_{\odot} yr^{-1}$ and the mass-loss rate for the old shell is $\sim 4.0 \times 10^{-6} M_{\odot} yr^{-1}$. The value for the newly-forming SiC determined from the present model for U Ant is $\sim 1.5 \times 10^{-8} M_{\odot} yr^{-1}$, whereas the mass-loss rate for the old shell is $\sim 2.4 \times 10^{-6} M_{\odot} yr^{-1}$. The agreement between these values is very good given the uncertainties in the dust-to-gas ratio and the CO to H_2 ratio.

Recent ISO-ISOPHOT observations of Y CVn (IRAS 12427+4542; see figure 3) at 90 μm and 160 μm have also confirmed the existence of the detached shell (Izumiuza et al. 1996). Y CVn is one of the candidates of the transition objects fitted well by the *interrupted mass-loss model*. The mass-loss rate of the new SiC shell determined from the present model is $\sim 4.6 \times 10^{-8} M_{\odot} yr^{-1}$, whereas the mass-loss rate for the old shell is $\sim 5.1 \times 10^{-7} M_{\odot} yr^{-1}$, The value of old shell determined by Izumiura et al. is $\sim 7 \times 10^{-6} M_{\odot} yr^{-1}$ The agreement between these values is good given uncertainties based on different input parameters.

5.2. The promise of first

Nevertheless, the observations of the double-peaked profiles by Olofsson et al. (1990, 1992, 1996) and Yamamura et al. (1993) as well as the clear detection of detached shell by Izumiura et al. (1996) provide strong support that these transition objects are in between two mass-loss phases of evolution.

FIRST mission will be played an important role for the detailed study of these objects. Three instruments, which are PACS (Photodetector Array Camera & Spectrometer), SPIRE (Spectral and Photometric Imaging REceiver) and HIFI (Heterodyne Instrument for FIRST), will be aboard FIRST, covering the wavelength range 60 μm – 670 μm. They will provide us the important information, which ISO and IRAS could not provide us currently, to further study the nature of carbon stars.

Acknowledgements

S. J. Chan thanks the Program Organizing Committee of the Promise of FIRST conference for offering her travel grant to attend the conference.

References

Chan, S.J. Kwok, S. 1988, ApJ, 334, 362

Chan, S.J. Kwok, S. 1990, A&A, 237, 354

Chan, S.J. 1992, Ph.D. Thesis, University of Calgary, Canada

Chan, S.J.,1993, PASP, 105, 1107

Egan, M.P., Leung, C.M., Spagna, G.F.Jr. 1988, Comput. Phys. Comm., 28, 337

Epchtein, N., Le Bertre, T., Lépine, J.R.D., Marques dos Santos, P., Matsuura, O.T., and Picazzio, E. 1987, A&AS, 71, 39

Epchtein, N., Le Bertre, T., Lépine, J.R.D., 1990, A&AS, 227, 82

Gezari D.Y., et al. 1994, Catalogue of Infrared Observations, NASA (On-line version)

Hoffleit, D., Jascheck, C., 1982, The Bright Star Catalog, 4th revised ed. (New Haven, Yale University Observatory)

Noguchi, K., Kawara, K., Kobayashi, Y., Okuda, H., Sato, S., Oishi, M. 1981, PASJ, 33, 372

Izumiura, H., Hashimoto, O., Kawara, K., Yamanura, I., Waters, L.B.F.M. 1996, A&A, 315, L221

Noguchi, K., Murakami, H., Matsuo, H., Noda, M., Hamada, H., Watabe, T. 1990, PASJ, 42, 441

Olofsson, H., Carlstom, U., Eriksson, K., Gustafsson, B., Wilson, L.A. 1990, A&A, 230, L13

Olofsson, H., Carlstom, U., Eriksson, K., Gustafsson, B., Wilson, L.A. 1992, A&A, 253, L17

Olofsson, H., Bergman, H., Eriksson, K., Gustafsson, B. 1996, A&A, 311, 587

Price, S.D., Walker, R.D. 1976, The AFGL Four Color Infrared Sky Survey, Air Force Geophys. Lab. Tech. Rep. No. AFGL TR-76-0208

Stephenson, C.B. 1989, A General Catalog of Cool Galactic Carbon Stars, 2nd ed., Publ. Warner & Swasey Obs., 3, No. 2

Thronson, H.A., Latter, W.B., Black, J.H., Bally, J., Hacking, P. 1987, ApJ, 322, 770